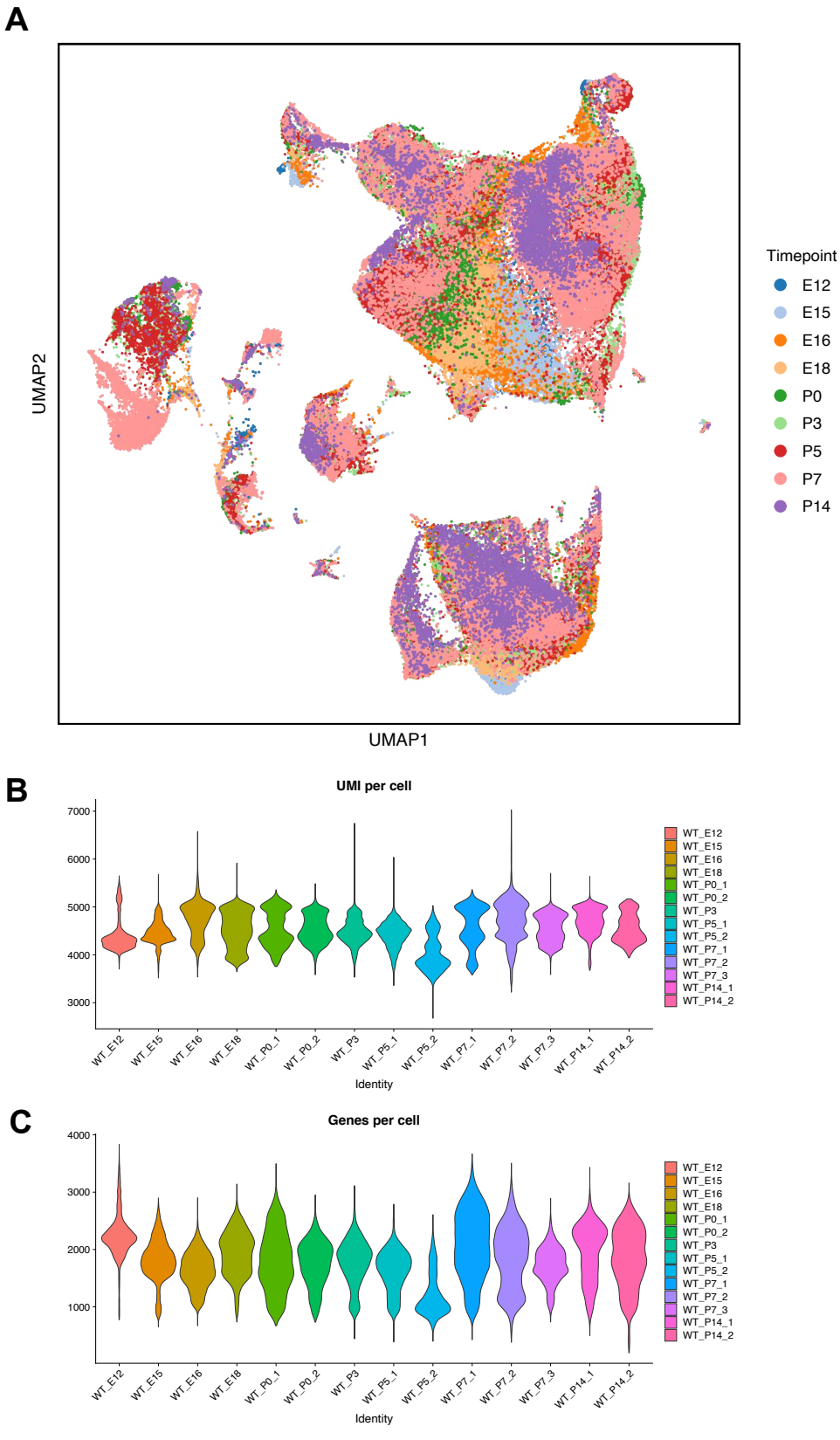

Fig. S1. A time course of single-cell transcriptomes from the developing mouse lung was collected. **A)** UMAP of all sequenced cells colored by timepoint indicates that time plays a role in the cellular clustering. **B)** The number of UMIs (unique molecular identifiers) from each cell is plotted as a violin plot, grouped (by color) per sequencing run. **C)** A similar plot is presented for the number of genes (with a UMI > 1) that were detected per cell.

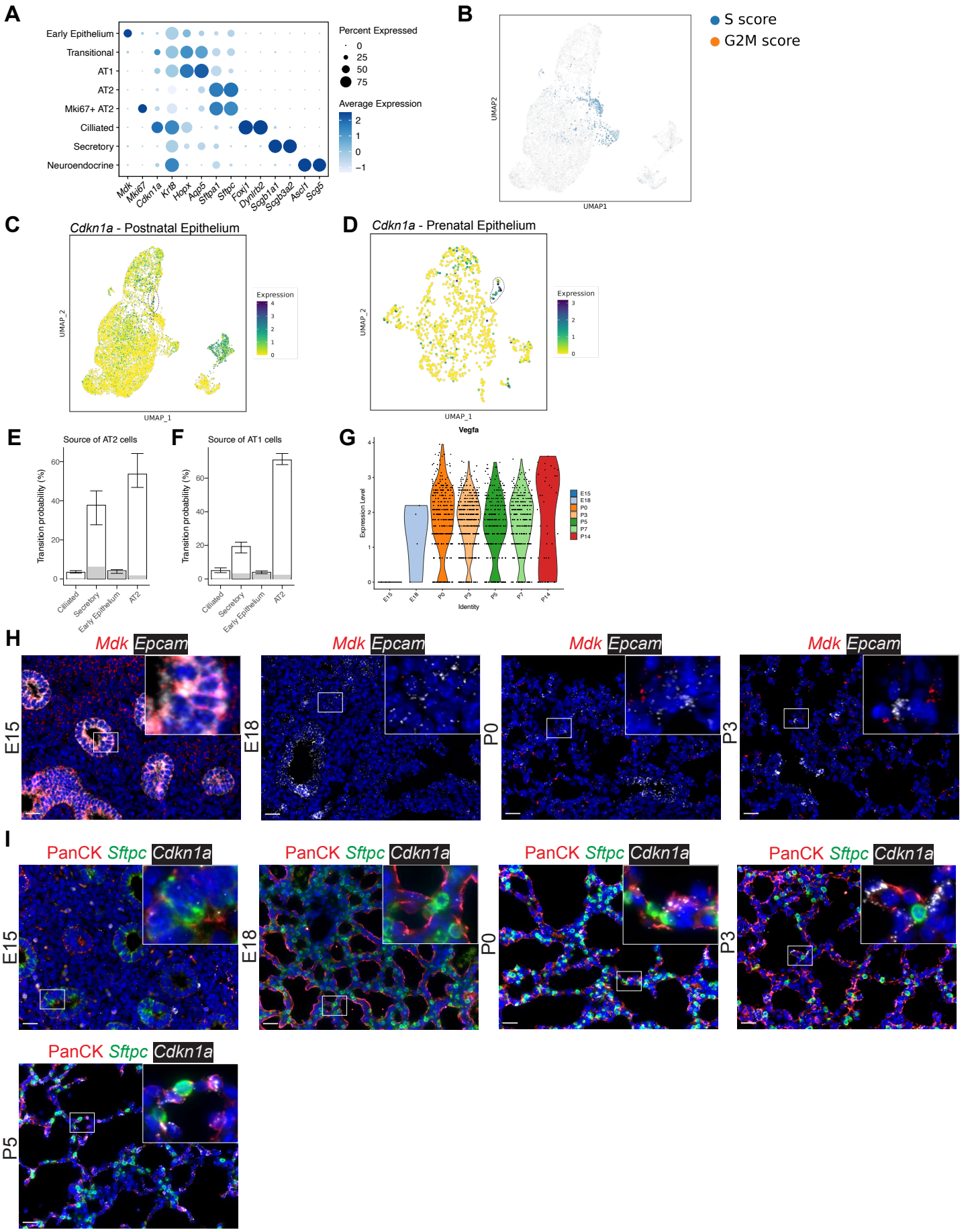

Fig. S2. scRNAseq of the developing lung epithelium identifies the appearance of distinct cell types by E18. **A)** Clusters were assigned to cell types based on established hallmark gene expression. Marker gene expression by cluster is displayed in a dot plot, where higher expression is represented as a darker color. The size of the dot indicates the proportion of cells expressing that marker. **B)** Cell-cycle score analysis (a multi-gene metric) was performed with scVelo and plotted on a UMAP embedding. The darker the color, the greater the S or G2M cell-cycle score. **C)** UMAP embedding of the prenatal epithelium colored by cell type, where the transitional cells are circled. **D)** UMAP embedding of the prenatal epithelium where individual cells are colored by the expression of *Cdkn1a*. **E-F)** Cell-trajectory inference was calculated with CellRank based on RNA expression profiles and RNA velocity to predict the source of **E)** AT2 cells and **F)** AT1 cells. **G)** A violin plot of *Vegfa* expression in AT1 cells, grouped by time. **H)** RNA in situ hybridization was used to identify cells expressing *Mdk* (red) and *Epcam* (white, epithelial-cell marker). **I)** Immunofluorescence and RNA in situ hybridization identified cells that are expressing PanCK (pan-cytokeratin, red, epithelial-cell marker), *Sftpc* (green, AT2-cell marker), and *Cdkn1a* (white, transitional-cell marker). Scale bar = 25 μm.

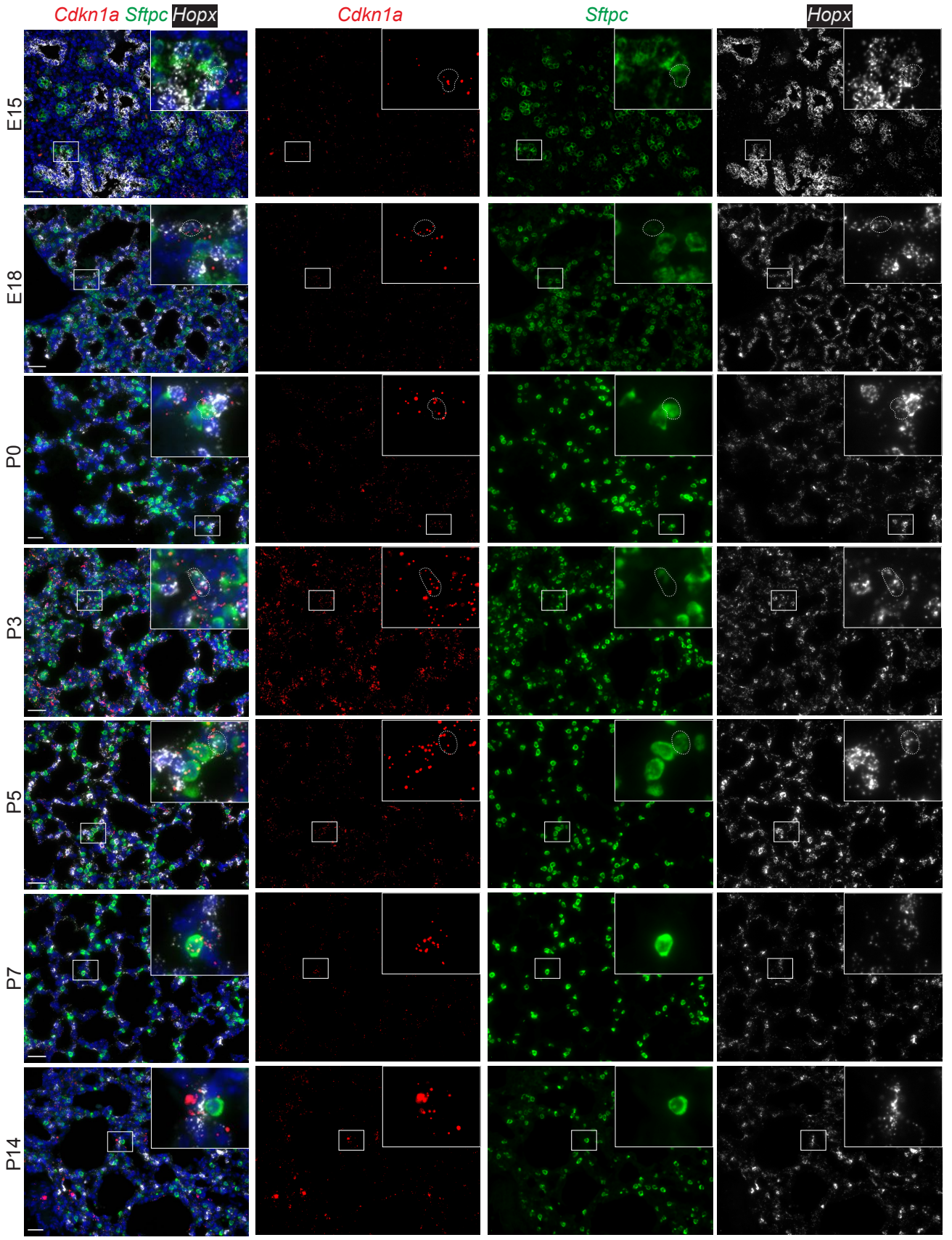

Fig. S3. Transitional epithelial cells are identified by expression of *Cdkn1a*. RNA in situ hybridization was used to identify cells expressing *Cdkn1a* (red, transitional-cell marker), *Sftpc* (green, AT2-cell marker) and *Hopx* (white, AT1-cell marker). Images are separated by channel. Cells that are positive for all three markers are circled with a dashed line Scale bar = 25 μm.

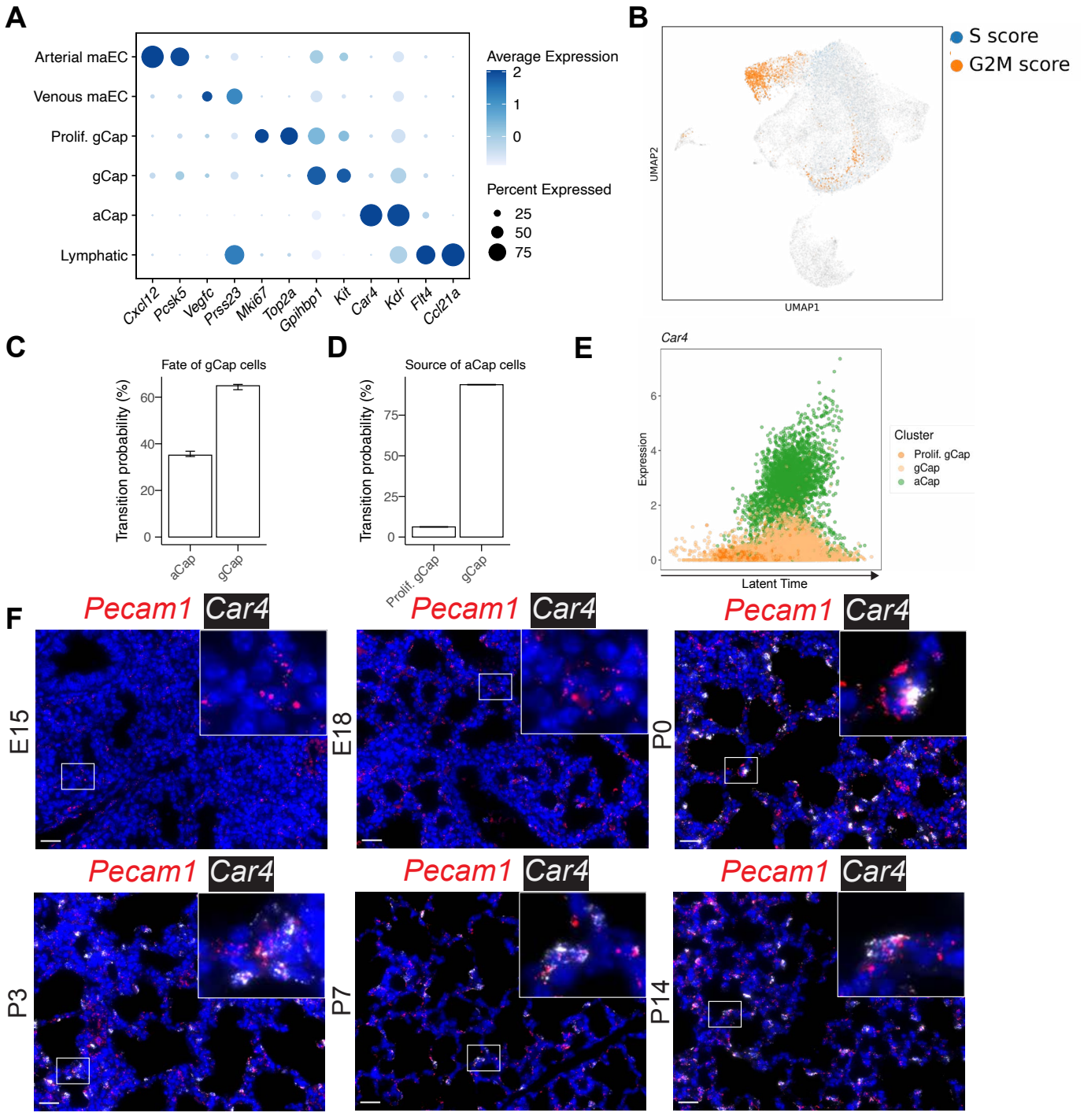

Fig. S4. scRNA-seq of the developing lung endothelium identifies early population stability, and an appearance of *Car4*+ cells at E18. **A)** Clusters were assigned to cell types based on known marker gene expression. Marker gene expression by cluster is displayed in a dot plot, where higher expression is represented as a darker color. The size of the dot indicates the proportion of cells expressing that marker. **B)** Cell-cycle score analysis (a multi-gene metric) was performed with scVelo and plotted on a UMAP embedding. The darker the color, the greater the S or G2M cell-cycle score. **C-D)** Cell-trajectory probability was calculated with CellRank based on RNA expression profiles and RNA velocity to predict the trajectory of **D)** gCap cells and the trajectory of **E)** aCap cells. **F)** RNA in situ hybridization was used to identify cells expressing *Pecam1* (red, endothelial-cell marker) and *Car4* (white, aCap cell marker). Scale bar = 25 μm.

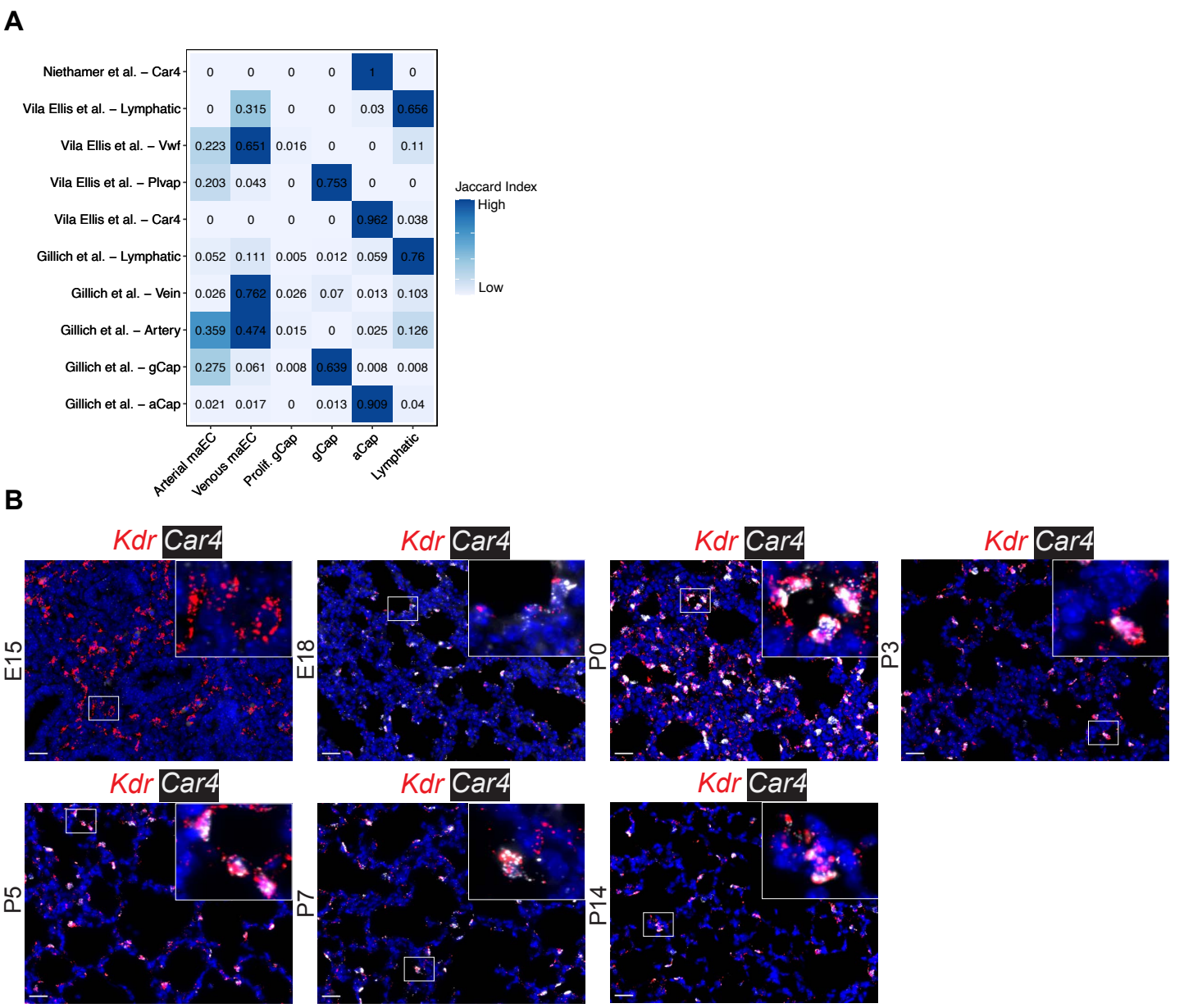

Fig. S5. Endothelial cell clusters resemble those previously described, and *Kdr* expression is enriched in aCap cells. **A)** A Jaccard index was calculated between clusters identified in this study and clusters identified in other studies. The intensity of color indicates relative similarity, with darker colors indicating higher similarity. A row-normalized Jaccard index is indicated. **B)** RNA in situ hybridization was used to identify cells that are expressing *Kdr* (red) and *Car4* (white, aCap cell marker). Scale bar = 25 µm.

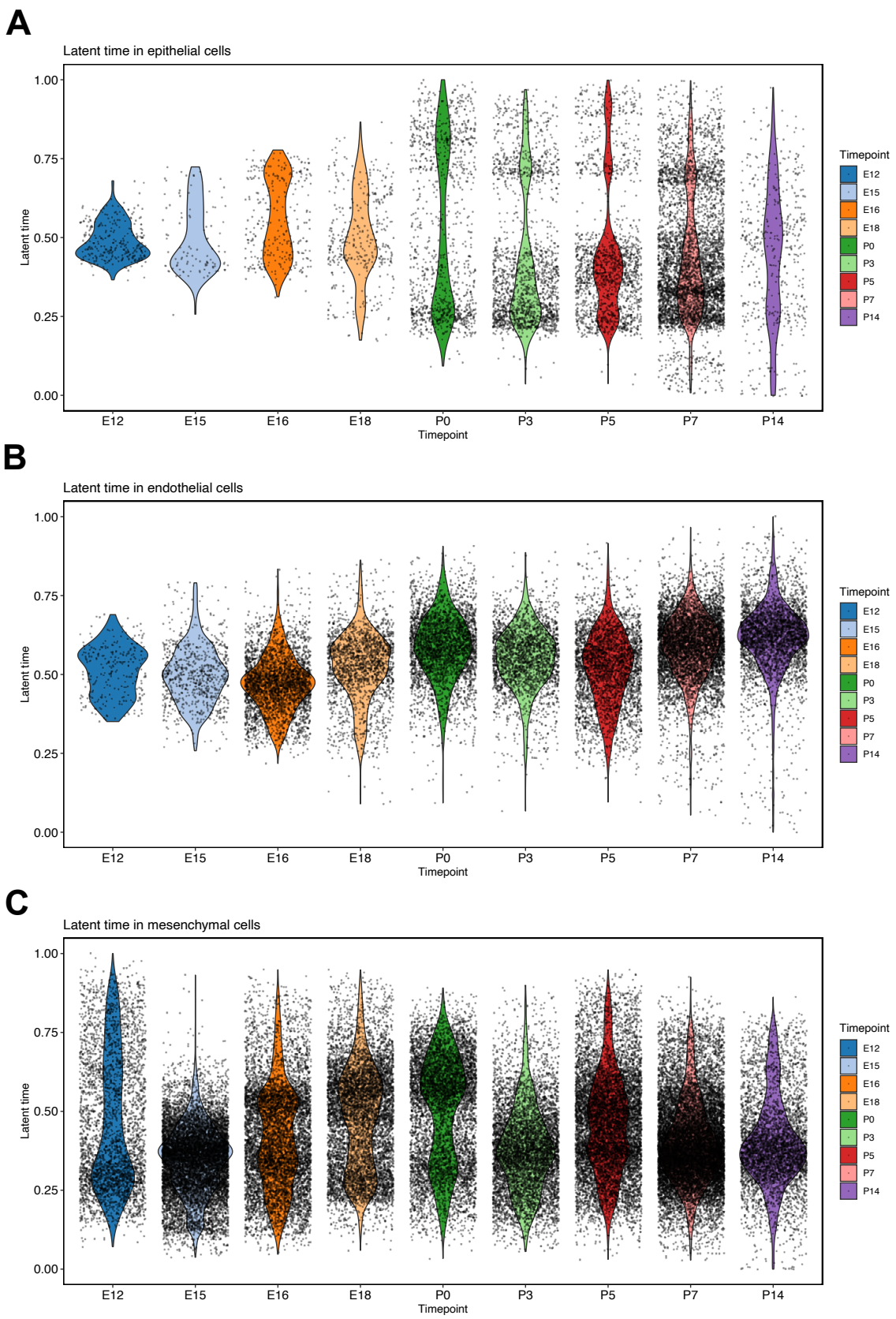

Fig. S6. Latent time only broadly corresponds with developmental time. Latent time (a proxy for cellular maturity) was calculated for each cell using CellRank and plotted in a violin plot that is grouped by developmental timepoint. Plots were made for all cells in the **A)** epithelium, **B)** endothelium, and **C)** mesenchyme. Dots represent the latent time values of individual cells.

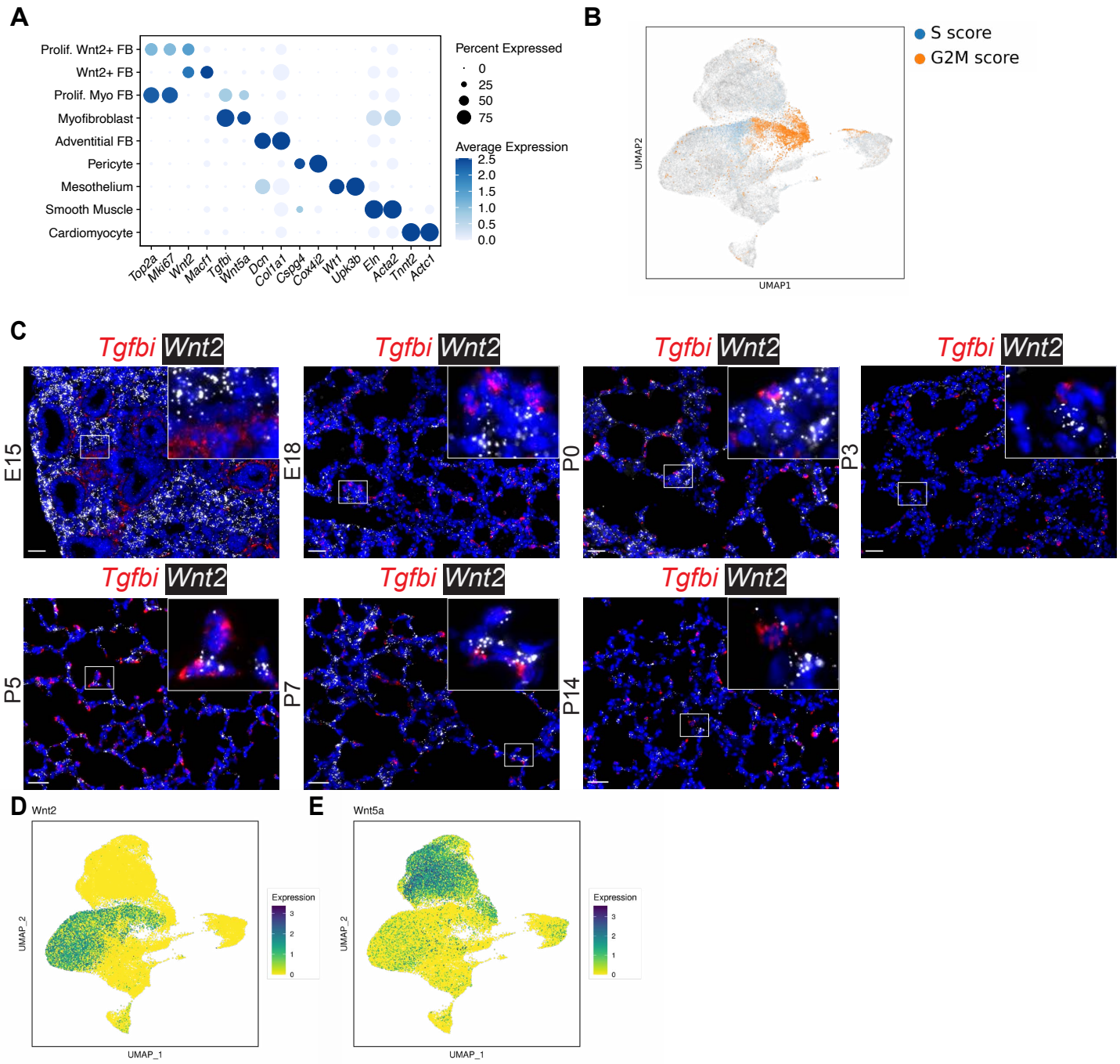

Fig. S7. scRNA-seq of the developing lung mesenchyme identifies broad changes over developmental time. **A)** Clusters were assigned to cell types based on known marker gene expression. Marker gene expression by cluster is displayed in a dot plot, where higher expression is represented as a darker color. The size of the dot indicates the proportion of cells expressing that marker. **B)** Cell-cycle score analysis (a multi-gene metric) was performed with scVelo and plotted on a UMAP embedding. The darker the color, the greater the S or G2M cell cycle score. **C)** RNA in situ hybridization (ISH) identified cells expressing *Tgfbi* (red, myofibroblast marker) and *Wnt2* (white, *Wnt2*+ fibroblast marker). Scale bar = 25 μm. **D)** UMAP embedding where individual cells are colored by the expression of *Wnt2* and **E)** *Wnt5a*.

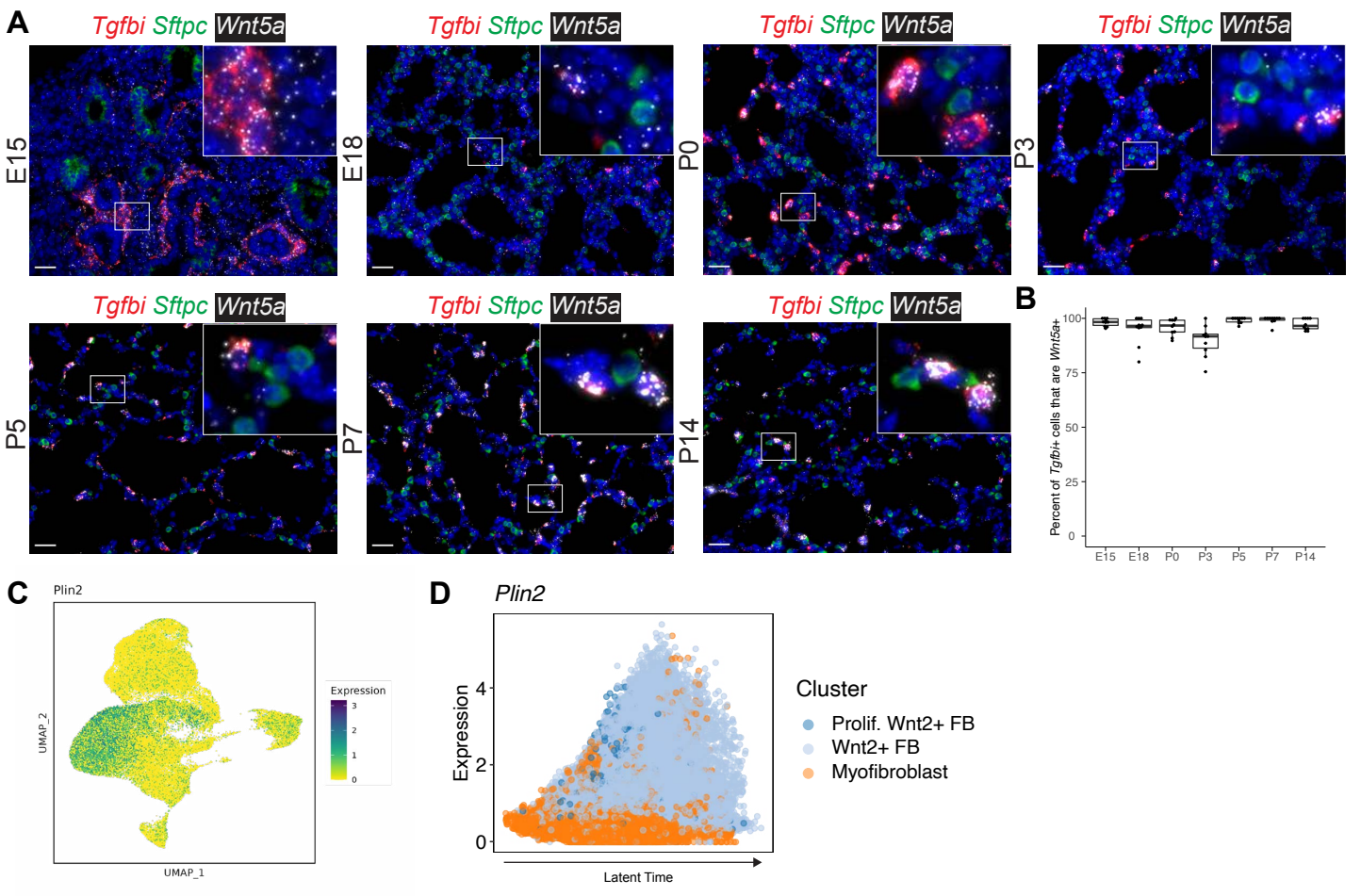

Fig. S8. *Tgfbi*+ myofibroblasts express *Wnt5a* after E15. **A)** RNA in situ hybridization (ISH) was used to identify cells expressing *Tgfbi* (red, myofibroblast marker), *Sftpc* (green, AT2-cell marker), and *Wnt5a* (white). Scale bar = 25 µm. **B)** Quantification of ISH was performed using HALO and the percentage of *Tgfbi*+ cells that are *Wnt5a*+ was plotted. Boxplots represent the summary data and each dot represents the percentage of *Tgfbi*+*Wnt5a*+ / *Tgfbi*+ cells per image. **C)** UMAP embedding where individual cells are colored by the expression of *Plin2*. **D)** Latent time analysis, where latent time increases along the *x*-axis, shows expression of *Plin2* in *Wnt2*+ fibroblasts.

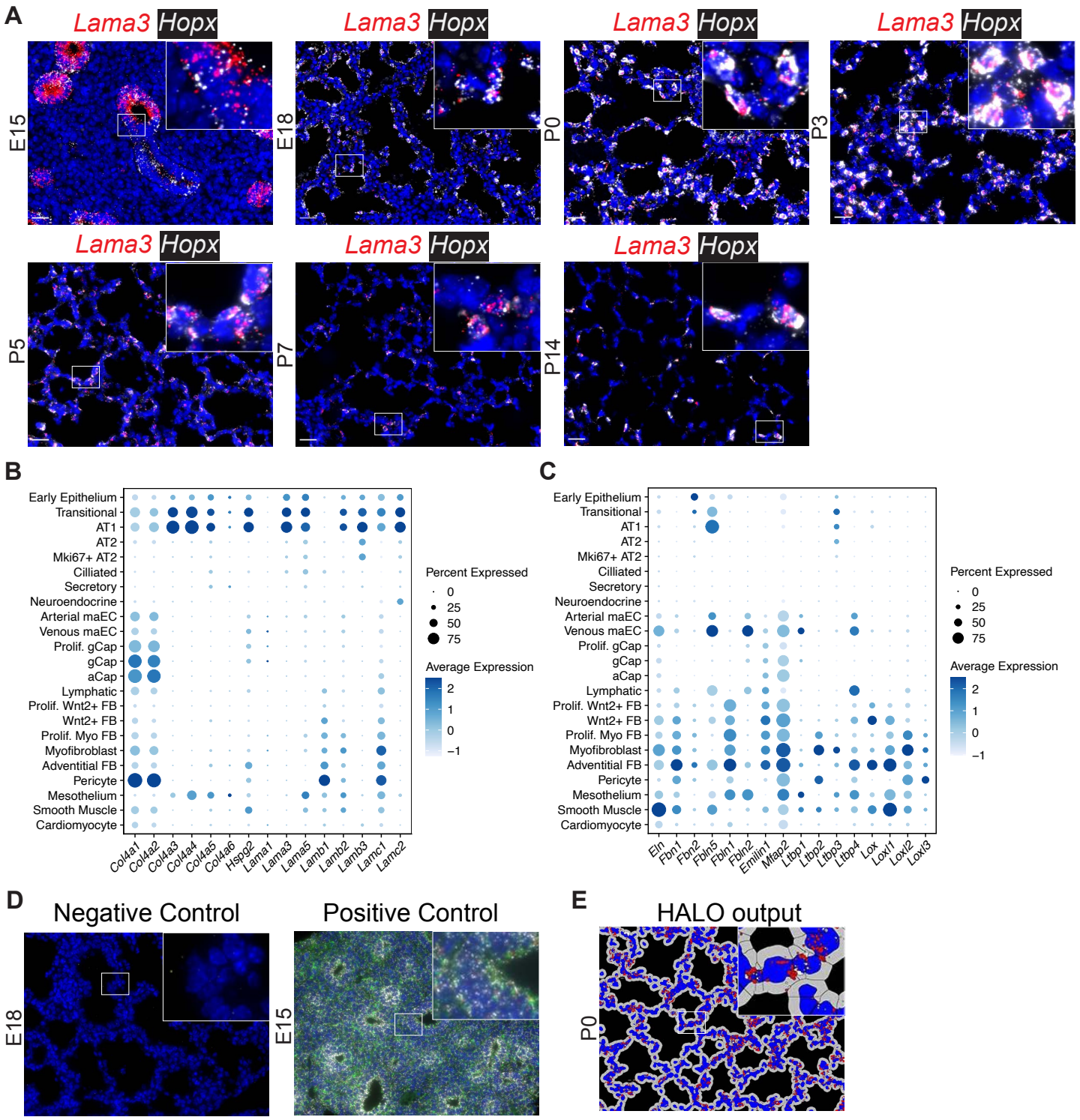

Fig. S9. AT1 cells marked by *Hopx* express *Lama3* throughout development. **A)** RNA in situ hybridization (ISH) was used to identify cells that are expressing *Lama3* (red), and *Hopx* (white, AT1-cell marker). Scale bar = 25 µm. **B)** Dot plot showing gene expression of basement membrane related genes in every cluster of cells at all timepoints. The color intensity of the circles indicates the expression level. The size of the dot indicates the proportion of cells expressing that marker. **C)** Dotplot of elastin-related genes in every cluster of cells at all timepoints. **D)** All ISH experiments were accompanied with slides stained with positive and negative controls; a representative image of each is presented here. Both images were captured with identical exposure settings. **E)** HALO automated image-analysis software (Indica Labs) was used for analysis of all ISH images. An example of HALO output for the P0 in panel A above is shown.

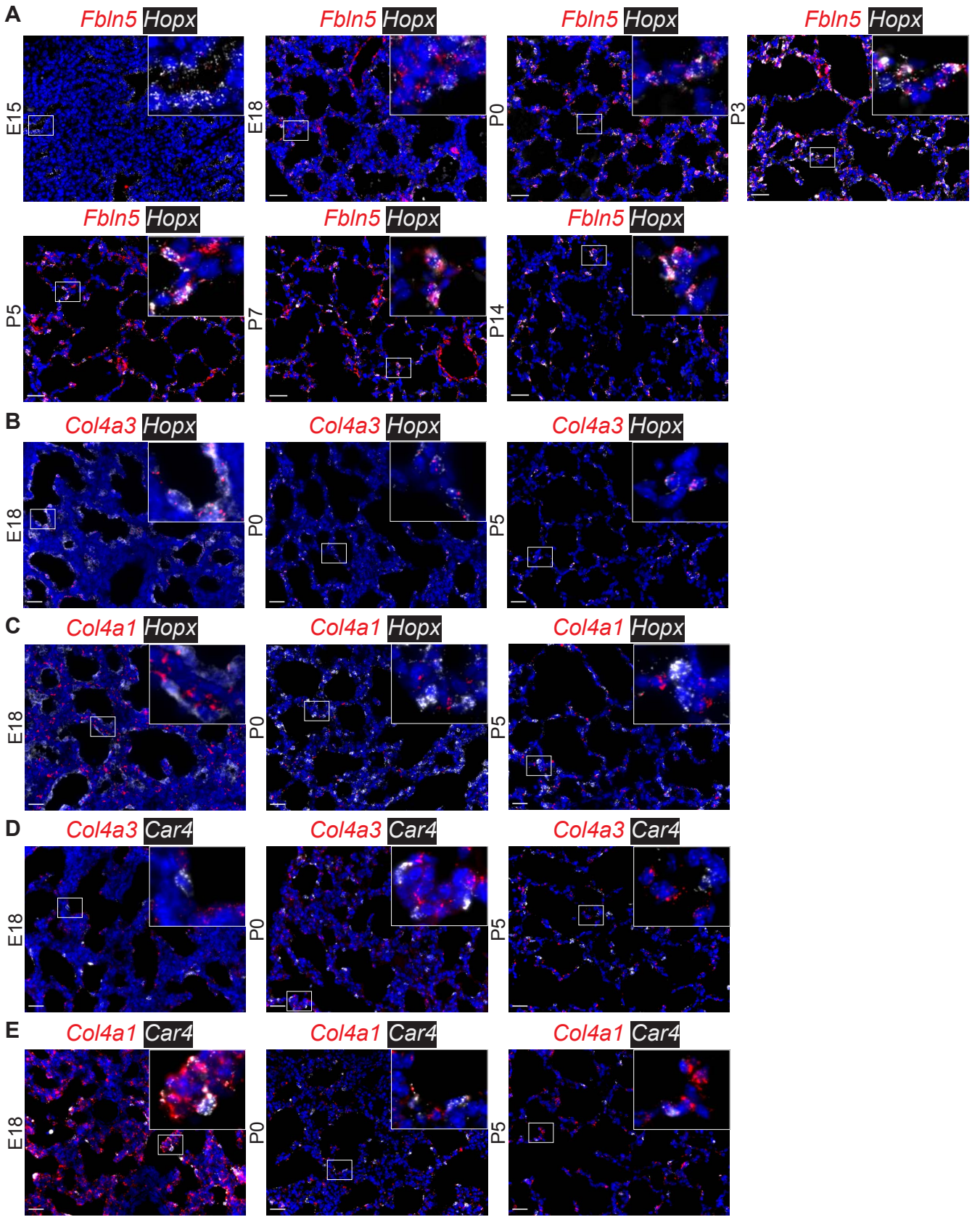

Fig. S10. RNA in situ hybridization was used to identify extracellular matrix expression patterns in AT1 (marked by *Hopx*) and aCap (marked by *Car4*) cells. Cellular localization patterns were evaluated for **A)** *Fbln5* (red) and *Hopx* (white), **B)** *Col4a3* (red) and *Hopx* (white), **C)** *Col4a1* (red) and *Hopx* (white), **D)** *Col4a3* (red) and *Car4* (white), and **E)** *Col4a1* (red) and *Car4* (white).

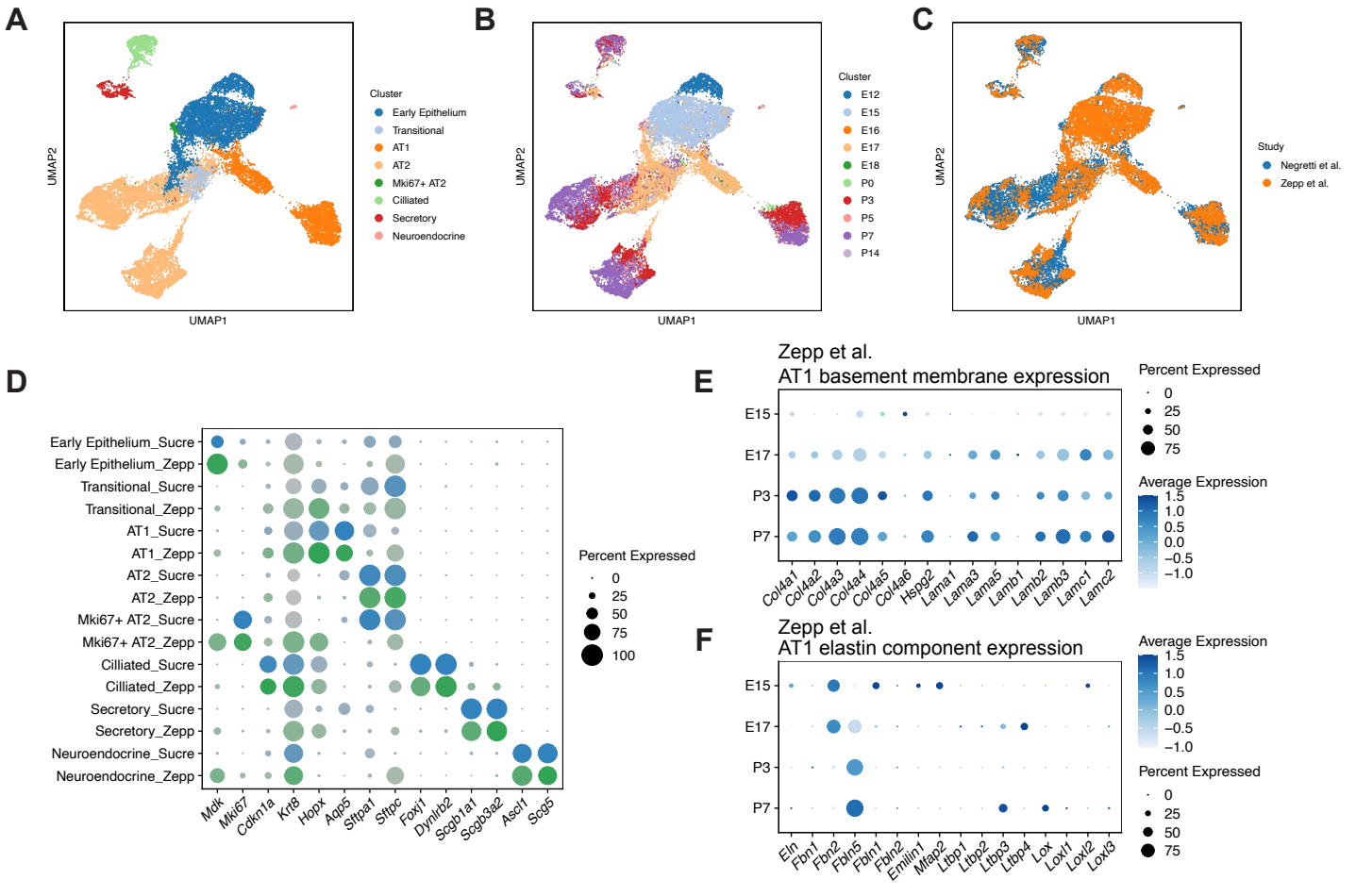

Fig. S11. Data from epithelial cells gathered in this study were jointly analyzed with epithelial cells from Zepp et al. 2021. Clustering of the joint dataset after integration indicates highly similar clustering, with all cell types identified here being present in the Zepp et al. dataset. **A)** UMAP of joint data colored by cell type. **B)** UMAP of joint data colored by timepoint. **C)** UMAP of joint data colored by study. **D)** Marker gene expression for the epithelial clusters is plotted in a heatmap, where darker colors indicate higher expression. The size of the dot indicates the proportion of cells that are expressing those genes. Dots are colored by study. **E)** Expression of basement membrane components was assessed in AT1 cells from the Zepp et al. study. **F)** Expression of elastin components was assessed in AT1 cells from the Zepp et al. study.

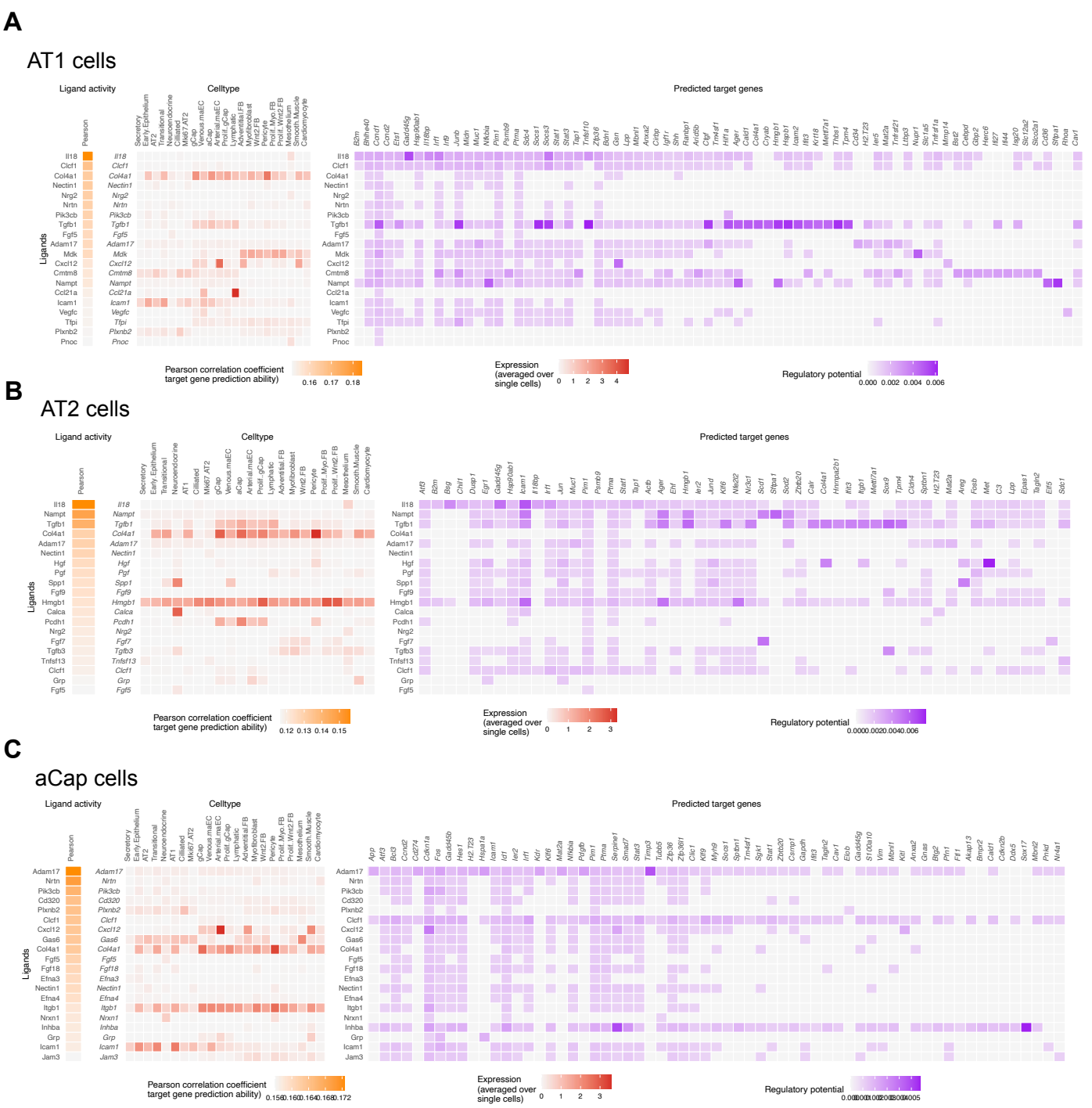

Fig. S12. To assess potential cell-cell communication, specific cell types were assessed with NicheNet. Genes that were different between saccular (P0, P3) and alveolar (P7, P14) stages were used as the 'responsive' genes, and every other cell type in the dataset was considered a potential sender. Three heatmaps were constructed (left to right) displaying the predicted ligand activity (orange), the expression of the predicted ligand in specific cell types (red), and the predicted regulatory potential of the ligand on downstream targets in selected cell types (purple). NicheNet analysis is presented for selected cells in the alveolar space: **A)** AT1 cells, **B)** AT2 cells, and **C)** aCap cells.

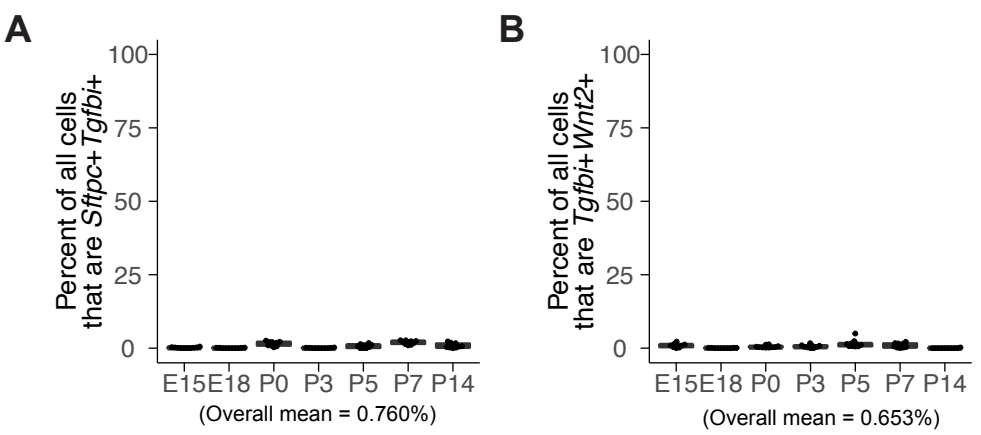

Fig. S13. The rate of false-positive colocalization detection was assessed in RNA in situ hybridization images after HALO analysis. The non-physiological combinations of **A)** *Wnt5a*+ and *Sftpc*+ cells, and **B)** *Wnt2*+ and *Tgfbi*+ cells were tested. The overall mean rate of false double positive detection was < 1%.

Table S1. Marker genes organized by each cluster of cells.

Click here to download Table S1

Table S2. Relative cell numbers that are compared with cellular proportion by RNA *in situ* hybridization, or by scRNA-seq.

Click here to download Table S2

Table S3. Genes that have expression profiles that significantly change over developmental time, organized as indicated in the heatmaps in Fig. 2D-F.

Click here to download Table S3

Table S4. Gene expression in the endothelium that is correlated with the aCap fate probability.

Click here to download Table S4